

See discussions, stats, and author profiles for this publication at: <https://www.researchgate.net/publication/225271771>

# Reaction of Nerve Agents with Phosphate Buffer at pH 7

ARTICLE *in* THE JOURNAL OF PHYSICAL CHEMISTRY A · JUNE 2012

Impact Factor: 2.69 · DOI: 10.1021/jp3024809 · Source: PubMed

---

CITATIONS

3

---

READS

64

3 AUTHORS, INCLUDING:



William Creasy

SAIC

54 PUBLICATIONS 937 CITATIONS

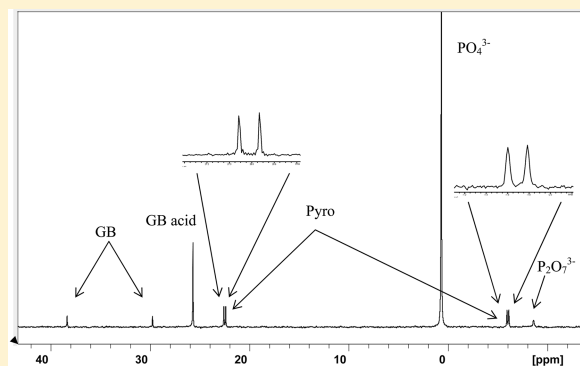
SEE PROFILE

## Reaction of Nerve Agents with Phosphate Buffer at pH 7

William R. Creasy,<sup>\*,†</sup> Roderick A. Fry,<sup>‡</sup> and David J. McGarvey<sup>‡</sup><sup>†</sup>SAIC, P.O. Box 68 Gunpowder Branch, Aberdeen Proving Ground, Maryland 21010, United States<sup>‡</sup>Edgewood Chemical Biological Center, Aberdeen Proving Ground-Edgewood Area, Maryland 21010, United States

## S Supporting Information

**ABSTRACT:** Chemical weapon nerve agents, including isopropyl methylphosphonofluoridate (GB or Sarin), pinacolyl methylphosphonofluoridate (GD or Soman), and S-(2-diisopropylaminoethyl) O-ethyl methylphosphonothioate (VX), are slow to react in aqueous solutions at midrange pH levels. The nerve agent reactivity increases in phosphate buffer at pH 7, relative to distilled water or acetate buffer. Reactions were studied using <sup>31</sup>P NMR. Phosphate causes faster reaction to the corresponding alkyl methylphosphonic acids, and produces a mixed phosphate/phosphonate compound as an intermediate reaction product. GB has the fastest reaction rate, with a bimolecular rate constant of  $4.6 \times 10^{-3} \text{ M}^{-1}\text{s}^{-1} [\text{PO}_4^{3-}]$ . The molar product branching ratio of GB acid to the pyro product (isopropyl methylphosphonate phosphate anhydride) is 1:1.4, independent of phosphate concentration, and the pyro product continues to react much slower to form GB acid. The pyro product has two doublets in the <sup>31</sup>P NMR spectrum. The rate of reaction for GD is slower than GB, with a rate constant of  $1.26 \times 10^{-3} \text{ M}^{-1}\text{s}^{-1} [\text{PO}_4^{3-}]$ . The rate for VX is considerably slower, with a rate constant of  $1.39 \times 10^{-5} \text{ M}^{-1}\text{s}^{-1} [\text{PO}_4^{3-}]$ , about 2 orders of magnitude slower than the rate for GD. The rate constant of the reaction of GD with pyrophosphate at pH 8 is  $2.04 \times 10^{-3} \text{ min}^{-1}$  at a concentration of 0.0145 M. The rate of reaction for diisopropyl fluorophosphate is  $2.84 \times 10^{-3} \text{ min}^{-1}$  at a concentration of 0.153 M phosphate, a factor of 4 slower than GD and a factor of 15 slower than GB, and there is no detectable pyro product. The half-lives of secondary reaction of the GB pyro product in 0.153 and 0.046 M solution of phosphate are 23.8 and 28.0 h, respectively, which indicates little or no dependence on phosphate.



## ■ INTRODUCTION

Chemical weapon (CW) nerve agents, including isopropyl methylphosphonofluoridate (GB or Sarin), pinacolyl methylphosphonofluoridate (GD or Soman), and S-(2-diisopropylaminoethyl) O-ethyl methylphosphonothioate (VX), are highly toxic cholinesterase inhibitors that react slowly in aqueous solutions at midrange pH levels (6.5–7.5). The hydrolysis rate of VX at 25 °C is reported by Epstein and co-workers as  $7 \times 10^{-4} \text{ hr}^{-1}$ , or a half-life of 41 days.<sup>1</sup> Somani reports the half-life of VX as 350 days at 25 °C, and the half-life of GB as 5.4 h.<sup>2</sup> The Organization for the Prohibition of Chemical Weapons (OPCW) reports the half-lives of VX and GB as about 200 days and 8 days, respectively, at 25 °C.<sup>3</sup> Munro et al. reports that the half-life for VX in water at 25 °C and pH 7 ranges from 17 to 42 days; for GB at 25 °C, the half-life ranges from 237 h (pH 6.5) to 24 h (pH 7.5); and GD has an estimated half-life of approximately 60 h at pH 6 and 25 °C.<sup>4</sup>

GB has perhaps been studied in the most detail with regard to hydrolysis<sup>5–7</sup> and other displacement reactions,<sup>8</sup> including reactions with hypochlorite,<sup>7</sup> amines,<sup>9</sup> metal ions,<sup>10</sup> catechols,<sup>11</sup> and phenols.<sup>12,13</sup> Hydrolysis rates seem to be affected by high concentration of anions even if they are not strongly reactive.<sup>14</sup>

Studies are being done for testing of various CW decontamination solutions,<sup>15–18</sup> buffered enzymes,<sup>19–21</sup> solid formulations,<sup>22–25</sup> or catalyst solutions,<sup>11</sup> some at midrange pH

values. These efforts are usually designed to develop less corrosive decontamination methods for CW agents as alternatives to strongly basic or oxidizing solutions that damage substrate materials, such as polymers and electronics. Studies are also underway of the reactions and degradation of CW agents in the environment after exposure to materials such as concrete, landfills, and marine environments.<sup>4,26–29</sup> These types of reactions are important in the various complex matrices in the event of a CW agent release into the environment. Studies of the stability of CW agents in simple aqueous solutions have also been reported.<sup>30</sup> A recent review by Churchill and co-workers provides the recent work on reactions in decontamination and environmental matrices.<sup>31</sup>

Reactions of nerve agents in phosphate buffers are important for physiological studies of nerve agent exposures and for the stability of standards prepared in phosphate buffers. Nerve agent reactivity has been previously observed to increase in phosphate buffer at pH 7 relative to distilled water or acetate buffer. Gáb and co-workers used a one-dimensional <sup>1</sup>H–<sup>31</sup>P heteronuclear single quantum coherence (1D <sup>1</sup>H–<sup>31</sup>P HSQC) experiment to detect reaction products of GB and GD in

Received: March 14, 2012

Revised: June 4, 2012

Published: June 5, 2012

phosphate solution.<sup>32</sup> Previous studies showed a lack of stability of GD in phosphate buffer solutions.<sup>33,34</sup> Buckles reported in 1947 that GD is hydrolyzed in less than 1 h in a solution of 0.2 M disodium phosphate/0.1 M citric acid at pH 7.4 and 37 °C, measured by titrating HF.<sup>35</sup>

Reactions of VX to form symmetrical pyrophosphonates by reaction with ethyl methylphosphonic acid are well-known,<sup>36,37</sup> as well as in the presence of water or peroxide.<sup>8</sup> In this study, the kinetics of the reactions of the nerve agents with aqueous phosphate buffer at pH 7 were measured, and the products are reported. Preliminary results from this study were reported previously.<sup>38</sup>

## ■ EXPERIMENTAL SECTION

Aqueous solutions were made with distilled, deionized water (DI water, CAS No. 7732-18-5, produced on demand using an in-house source from Barnstead, Inc.) and a stock solution of phosphate that was pH 7.0 ± 0.1. The composition of the stock solution was 1.61 M PO<sub>4</sub><sup>3-</sup>, made from 87.38 g K<sub>2</sub>HPO<sub>4</sub> (Sigma Aldrich >98%, CAS No. 7758-11-4) and 41.04 g KH<sub>2</sub>PO<sub>4</sub> (EM Scientific, crystals, CAS No. 7778-77-0) in 500 mL DI water. The pH of the solution was measured to be 6.94, using a Thermo Orion model 370 pH meter with a PrePHEct electrode, model No. 9272BN, glass combination pH sure flow, calibrated with pH 4, 7, and 10 standard buffer solutions.

Most of the reaction solutions were generated by diluting this stock solution in DI water. Since the reactions are usually slow, an attempt was made to avoid introducing any other potential contaminants that could add competing reactions. However, for the most dilute solutions, it was found that the buffering capacity of the dilute buffer solution was not sufficient to neutralize the acid that was formed by the hydrolysis of the agents. The production of acid by the reaction caused the rate to change over time, causing curvature in the pseudo-first-order rate plot. To eliminate this effect, ammonium acetate buffer was used to generate a constant total buffering capacity of 0.1 M. A stock solution of 0.2 M ammonium acetate (JT Baker # 0599-08, CAS No. 631-61-8) was used for the solutions. The pH measured for the 0.2 M solution was 7.00. Reaction rates that are reported for some phosphate solutions were measured both with and without 0.1 M ammonium acetate solution for extra buffering, as discussed in the next section.

CW agents isopropyl methylphosphonofluoridate (Sarin or GB, [CAS 107-44-8]), pinacolyl methylphosphonofluoridate (Soman or GD, [CAS 96-64-0]), and S-(2-diisopropylaminoethyl) O-ethyl methylphosphonothioate (VX, [CAS 50782-69-9]) were obtained from the Chemical Agent Standard Analytical Reference Material (CASARM) program at the Edgewood Chemical Biological Center, Aberdeen Proving Ground, MD. The agent purities were determined by liquid NMR and confirmed by gas chromatography/thermal conductivity detection. Purities of GB, GD, and VX were 97, 97, and 95 wt %, respectively. All handling of the CWA was conducted in a chemical surety laboratory certified for supertoxic compounds. Diisopropyl fluorophosphate (DFP) was purchased commercially from Aldrich ([CAS 55-91-4], part number D12,600-4). **Caution: The neat nerve agent compounds are extremely toxic and must be handled in accordance with all applicable Federal laws and international treaties, using appropriate safety and security operating procedures.**

For kinetic studies, 1 μL of agent was added to a total of 500 μL of aqueous solution to make a 14 mM solution, using a 10

μL pipet. Varying concentrations of phosphate and buffer solution were added in a 5-mm NMR tube (Wilmad-LabGlass, Vineland, NJ, Part No. 527-PP-8) and vortexed to make the aqueous solution. An amount of 50 μL D<sub>2</sub>O was added as an NMR lock solvent. Reaction data was collected on a Bruker Avance 300 Nuclear Magnetic Resonance Spectrometer (NMR) using <sup>31</sup>P detection at a frequency of 131 MHz, using a quadrupole nucleus probe (QNP). Most of the reactions were slow, so the number of signal-averaging scans was adjusted to improve the signal-to-noise, particularly later in the runs when the reagent was low in concentration. The greater number of scans increased the total signal acquisition time, but the relaxation delay of each scan was not changed. Many of the kinetic points were collected with automated spectra acquisition spaced by the length of the run. The time value of each data point was determined from the computer clock time at the midpoint of the run. Other instrument parameters include: sweep width (SW), 400 ppm; center frequency (O1P), 25 ppm; excite angle, 30°; recovery delay, 10 s; proton decoupling; D<sub>2</sub>O solvent locking; and number of transform points, 32K. The probe temperature was controlled by a thermostat, which was externally calibrated according the manufacturer's instructions by using solutions of methanol and ethylene glycol.<sup>39</sup>

Confirmation of the identity of the reaction products was done by liquid chromatography/tandem mass spectrometry (LC/MS and LC/MS/MS). Analysis was done on an Agilent LC model 1100 system with a model 6490 triple quadrupole mass spectrometer. Electrospray ionization in either positive or negative ion mode was used. Gradient elution from 100% aqueous 0.05 M ammonium acetate solution to 50% methanol was used, with a Phenomenex Synergi Hydro RP column (150 mm × 2.0 mm × 0.4 μm, part number 00F-4375-B0).

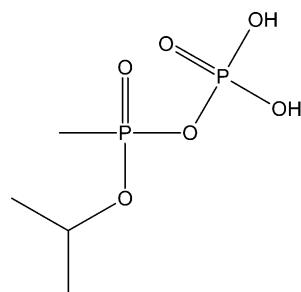
The NMR spectrum of the phosphate solution indicated that the solution contained a small amount of pyrophosphate at a chemical shift of -4.3 ppm. Since it was considered possible that the pyrophosphate was responsible for the observed reaction, a solution of pyrophosphate was made from reagent-grade sodium pyrophosphate basic decahydrate purchased from Sigma Aldrich (99.0%, [CAS 13472-36-1], part no. S6422-100G). A solution of 0.0145 M was prepared with 0.167 M ammonium acetate to decrease the pH to 8.0 and tested for reactivity.

## ■ RESULTS

**GB Reaction.** The reaction product from the hydrolysis of GB with water is isopropyl methylphosphonic acid (commonly called GB acid). In the presence of phosphate, the rate of reaction of GB to form GB acid is faster than in DI water or acetate buffer. The additional "pyro" product is observed that is a mixed phosphate/phosphonate compound identified as isopropyl methylphosphonate phosphate anhydride (structure 1), which reacts slowly. The compound is distinctive because of two widely spaced <sup>31</sup>P NMR doublets corresponding to the two distinct <sup>31</sup>P species, with the chemical shifts and coupling constants shown in Table 1. A sample NMR spectrum of a reaction mixture is shown in Figure 1. 1 has two doublets each with a small coupling from the <sup>31</sup>P-<sup>31</sup>P interaction of 22.3 Hz, consistent with NMR modeling results<sup>40</sup> and literature reports for the similar symmetric VX pyro compound bis[ethyl methylphosphonate]ester.<sup>41,42</sup>

Gäb and co-workers<sup>32</sup> used a 1D <sup>1</sup>H-<sup>31</sup>P HSQC experiment to detect the same reaction products of GB in phosphate

Structure 1. Pyro Reaction Product of GB and Phosphate

Table 1.  $^{31}\text{P}$  Chemical Shifts for Compounds in Aqueous pH 7 buffer<sup>a</sup>

compound	chemical shift (ppm)	coupling constant (Hz), proton decoupled
$\text{PO}_4^{3-}$ at pH 7 (mixture of protonated forms)	5.0	
GB	38.38	1045.5 ( $^{31}\text{P}$ – $^{19}\text{F}$ )
GB acid	30.02	
isopropyl methylphosphonate phosphate anhydride	26.8	22.2 ( $^{31}\text{P}$ – $^{31}\text{P}$ )
	–1.71	
pyrophosphate	–4.3	
GD	38.06	1047.5 ( $^{31}\text{P}$ – $^{19}\text{F}$ )
	37.41	
GD acid	29.0	
pinacolyl methylphosphonate phosphate anhydride	26.13, 25.86	21.4 ( $^{31}\text{P}$ – $^{31}\text{P}$ )
	–2.31, –2.34	21.5 ( $^{31}\text{P}$ – $^{31}\text{P}$ )

<sup>a</sup>Shifts are externally referenced to concentrated  $\text{H}_3\text{PO}_4$ .

solution. This technique works for molecules for which a  $^{31}\text{P}$  atom was within three bonds of a  $^1\text{H}$  nucleus, so the  $^{31}\text{P}$  from methylphosphonate is observed but the  $^{31}\text{P}$  from phosphate is not. This experiment had the advantage of greater sensitivity than 1D  $^{31}\text{P}$  NMR, so that lower concentrations of nerve agent and products could be detected. It has the disadvantages that  $^{31}\text{P}$  chemical shifts or coupling constants are not detected, and different compounds have different signal responses. In order to obtain kinetic information, the authors had to correct for the different signal responses of the reactants and products.

The semilog kinetic plot of GB hydrolysis in 0.1 M ammonium acetate buffer at pH 7 without phosphate is shown in Figure 2. The half-life calculated from the slope is

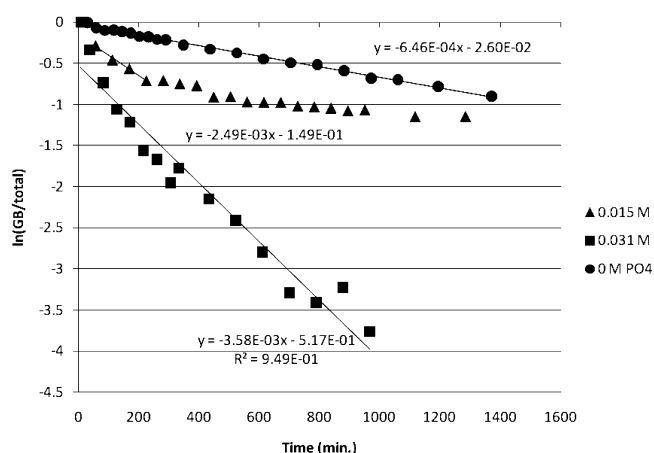


**Figure 2.** Semilog kinetic plot of the reaction of GB with and without  $\text{PO}_4^{3-}$  present. The half-life from the slope is calculated as 17.9 h for no phosphate buffer and 0.1 M acetate buffer. The reaction of GB in phosphate buffer at a concentration of 0.031 M  $\text{PO}_4^{3-}$  and 0.1 M acetate buffer has a half-life of 194 min. The half-life for 0.015 M  $\text{PO}_4^{3-}$  with no acetate buffer is 278 min, using only the first four data points. The curvature for the 0.015 M plot is due to the decreasing rate from the changing pH of the solution due to insufficient buffering of the acid reaction products.

17.9 h at 23 °C, which falls in the range of the previous reports of the GB reaction rate for pH 7 solution under these conditions. The y-axis of all the kinetic plots is the natural log of the ratio of molar concentration of remaining GB to the total of GB and products, including the pyro and acid products, using the signal from the  $^{31}\text{P}$  NMR. A question that was not studied is whether this slow reaction is affected by the use of a glass tube as a container, since the glass may react with the product HF as a sink to eliminate the reverse reaction. This issue could account for some of the variation in the reported rates of GB hydrolysis.

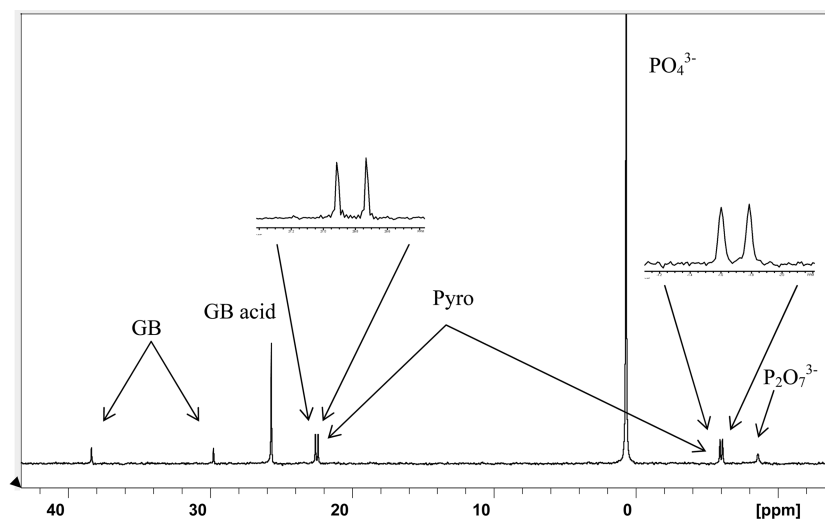


**Figure 1.** Sample NMR spectrum of GB and phosphate reaction solution, showing the residual reagent GB, the products GB acid and the pyro compound 1, and the reagent phosphate (partially protonated in solution) and impurity pyrophosphate (partially protonated in solution).

The rate increases substantially when phosphate was added, and it has linear dependence on phosphate concentration. The plot for GB in a 0.306 M phosphate buffer at 23 °C is shown in Figure 3. For this run only, 3  $\mu$ L of GB was added instead of 1

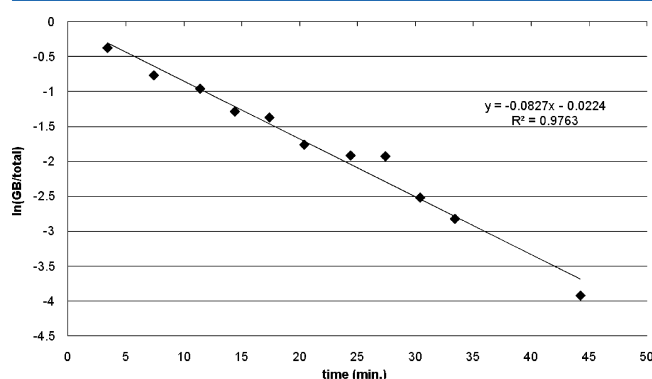


**Figure 3.** Semilog kinetic plot of the reaction of GB in phosphate buffer at a concentration of 0.306 M  $\text{PO}_4^{3-}$ . The half-life of the reaction is 8.4 min.

$\mu$ L, for a concentration of 42 mM, in order to increase the signal to use shorter runs, but this concentration is still in the pseudo-first-order condition. For these reaction conditions, the half-life is 8.4 min, or a factor of 140 times faster than in acetate buffer with no phosphate.

For the most dilute buffer solutions, it was found that the buffering capacity of the dilute phosphate solution was not sufficient to neutralize the acid that was formed by the hydrolysis of the agents. The rate is pH dependent, so a change in pH affects the rate, and the rate decreases from pH 7.5 to 6.5.<sup>4</sup> Acetate buffer was added to increase the buffer strength. Figure 2 shows the kinetic plots comparing reaction runs of GB in phosphate buffer with and without acetate buffer. The solutions have a concentration of 0.031 M  $\text{PO}_4^{3-}$  and 0.1 M acetate buffers, and 0.015 M  $\text{PO}_4^{3-}$  and no acetate buffer. The half-life of the reaction for 0.031 M  $\text{PO}_4^{3-}$  is 194 min. The half-life for 0.015 M  $\text{PO}_4^{3-}$  is 278 min, and only the first four data points are used since the plot curves as the reaction slows down. The curvature for the 0.015 M plot is due to the decreasing rate, caused by the changing pH of the solution due to insufficient buffering. By the end of the reaction, the pH of the solution was measured as pH 3 (using pH test paper).

A previous report by Ellin and co-workers<sup>43</sup> indicated that GB and GD in acetate buffer solution at pH 4.5 has faster degradation kinetics than other pH 4.5 buffer solutions, but the present results do not indicate that acetate promotes faster reaction at pH 7 compared to DI water, aside from buffering the solution so that the rate does not slow down.

In order to get a second-order rate constant, the reaction was done with a series of concentrations of phosphate. The plot of the pseudo-first-order rates versus phosphate concentration is shown in Figure 4. The bimolecular rate constant is found to be  $4.6 \times 10^{-3} \text{ M}^{-1} \text{ s}^{-1} [\text{PO}_4^{3-}]$  at 23 °C from the regression to this data. A data point in plotted using the kinetic data in ref 32.<sup>44</sup>

The product molar branching ratio of GB acid to **1** is 1:1.4 during the course of the reaction of GB, independent of the phosphate concentration. This ratio is in good agreement with the ratio reported by Gäb and co-workers for GB, GD, and GF.<sup>32</sup> The fact that the branching ratio does not change and does not depend on the phosphate concentration indicates that

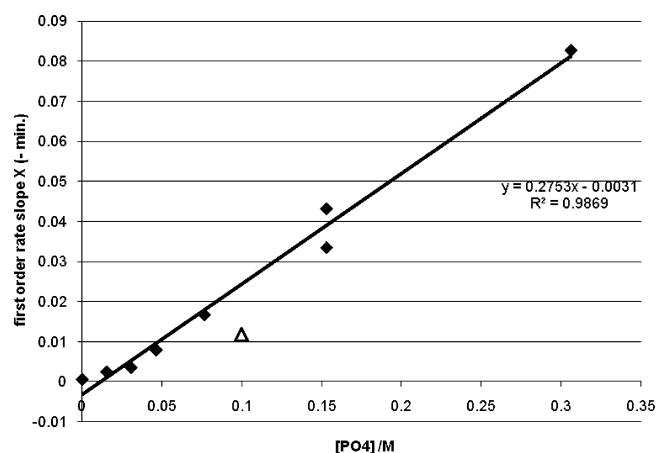


**Figure 4.** Linear plot of the first-order rates of GB reaction versus concentration of phosphate. All data is from this work, except  $\triangle$  from ref 32 (see text, not included in regression).

both products arise from a mechanism with a common intermediate. However, after the GB is consumed, **1** continues to react slowly to GB acid, discussed in a later section.

The temperature dependence of the reaction of GB with phosphate was measured at five temperatures from 23 to 63 °C, at a phosphate concentration of 0.0307 and 0.1 M acetate buffer. The rate data is plotted in Figure 5. The activation energy  $E_a$  that is found from the slope of the plot for the reaction is 63.3 kJ/mol.

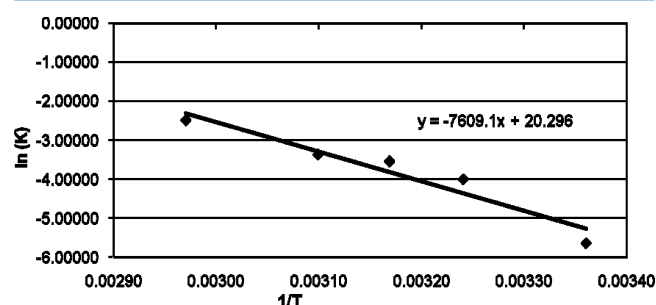


**Figure 5.** Rate data for the reaction of GB with phosphate at five temperatures, using the natural log of the rate constant of loss of GB at a concentration of 0.0307 M phosphate (with 0.1 M acetate buffer) versus reciprocal absolute temperature.

In order to confirm the identity of the product, the reaction solution was analyzed by LC/MS and LC/MS/MS. Products that were observed are given in Table 2 and are consistent with the assignment of the structure. In the positive ion electrospray mode, the  $[\text{M}+\text{H}]^+$  peak at  $m/z$  219 fragments to  $m/z$  177 with loss of propene, and to the  $m/z$  99 ion  $\text{H}_4\text{PO}_4^+$ . A minor peak at  $m/z$  137 corresponds to loss of  $\text{P}(\text{OH})_3$ . In the negative ion mode, the  $[\text{M}-\text{H}]^-$  peak at  $m/z$  217 fragments to form the

**Table 2.** LC/MS/MS Fragment Ions That Were Observed from Analysis of **1** and **2**

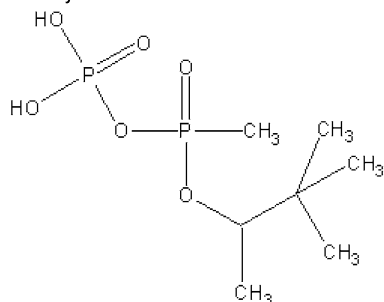
compound and polarity	parent ion, ( $m/z$ )	MS/MS fragment ions
<b>1</b> , positive ion	219	177, 137, 99
<b>1</b> , negative ion	217	79
<b>2</b> , positive ion	261	177, 99
<b>2</b> , negative ion	259	79



anion  $\text{CH}_3\text{P}(\text{OH})\text{O}^-$  or  $(\text{PO}_3)^-$  at  $m/z$  79. These results are in good agreement with those of Gäb and co-workers.<sup>32</sup>

**GD reaction.** GD has an analogous reaction to GB, but GD acid and structure 2 are formed. There is extra splitting of the

Structure 2. Pyro Reaction Product of GD and Phosphate



peaks for 2 in the NMR spectrum due to the diastereomers from two chiral centers, on the P atom and the pinacolyl C atom. Figure 6 shows the  $^{31}\text{P}$  NMR spectrum with expanded insets of the spectral lines. The peak shifts and coupling constants are given in Table 1.

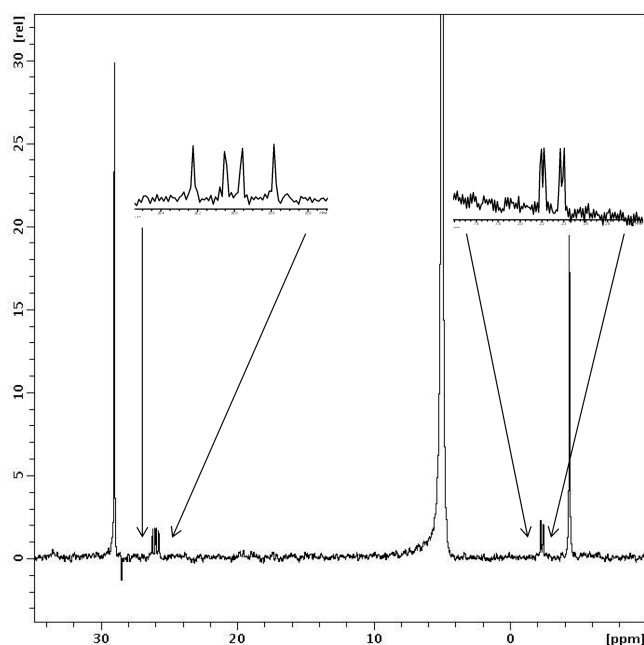


**Figure 6.** Product  $^{31}\text{P}$  NMR spectrum from GD reaction with phosphate, with insets showing the mixed pyro product, 2.

The semilog reaction rate plots of GD with phosphate in 0.1 M acetate buffer are linear. An example for 0.0766 M phosphate, with a half-life of 100.5 min, is given in the Supporting Information. The plot of the pseudo-first-order rates versus phosphate concentration is shown in Figure 7. The bimolecular rate constant is found to be  $1.26 \times 10^{-3} \text{ M}^{-1} \text{ s}^{-1}$   $[\text{PO}_4^{3-}]$ , which is 27% of the rate for GB. One data point for 0.1 M phosphate is plotted using the kinetic data in ref 32,<sup>44</sup> and one point for 0.02 M phosphate is plotted from ref 34.<sup>45</sup> These points were not used in the regression, but they are in good agreement to the best fit line. The rate of reaction for GD is probably slower than GB because of the greater steric hindrance of the pinacolyl group on the GD compared to the isopropyl group on the GB.

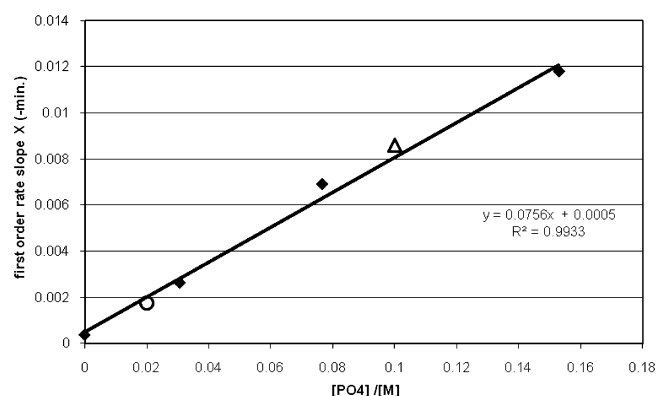


**Figure 7.** Linear plot of the first-order rates of GD reaction versus concentration of phosphate. All data is from this work, except  $\triangle$  from ref 32 and  $\circ$  from ref 34 (not included in regression).

In order to confirm the identity of the product, the reaction solution was analyzed by LC/MS and LC/MS/MS. Figure 8 shows the negative ion LC/MS spectrum, with the peaks at the expected masses. An interesting aspect of this spectrum is that sodium and potassium adduct ions were observed even in the negative ion spectrum, as  $[\text{M}+\text{Na}-2\text{H}]^-$ ,  $[2\text{M}+\text{Na}-2\text{H}]^-$ , and  $[2\text{M}+\text{K}-2\text{H}]^-$ . Fragment ions using LC/MS/MS are given in Table 2. As with 1, the  $[\text{M}+\text{H}]^+$  peak fragments to  $m/z$  177 with loss of alkene and to the  $m/z$  99 ion  $\text{H}_4\text{P}\text{O}_4^+$ . The  $[\text{M}-\text{H}]^-$  peak fragments to the anion  $\text{CH}_3\text{P}(\text{OH})\text{O}^-$  or  $(\text{PO}_3)^-$  at  $m/z$  79.

**GD Reaction with Pyrophosphate.** Since there was a 2.2 mol % of pyrophosphate impurity in the phosphate, it was considered that the source of the reaction could be from a fast reaction of agent with the low concentration of pyrophosphate. A solution of 0.0145 M pyrophosphate with 0.167 M ammonium acetate was made which was pH 8. The semilog kinetic plot for the reaction of GD with the solution of pyrophosphate is linear and is given in the Supporting Information. The rate constant of the reaction is  $2.04 \times 10^{-3} \text{ min}^{-1}$  at a concentration of 0.0145 M. The reaction rate of GD with phosphate at the same concentration, taken from the plot of Figure 7, is  $1.6 \times 10^{-3} \text{ min}^{-1}$ , only slightly slower. A pyro compound was observed in the NMR spectra, but the branching ratio of pyro/acid products is 10%, much lower than the reaction of GD with phosphate. As a result, the reaction of pyrophosphate does not significantly contribute to the production of 2. Since the concentration of pyrophosphate is much lower than phosphate in the pH 7 buffer solution, this reaction channel does not contribute significantly to the overall reaction rate.

**VX Reaction.** VX reacts with phosphate, but much slower than GD. The analogous mixed pyro product is observed in the  $^{31}\text{P}$  NMR spectra. The semilog reaction rate plot for the VX reaction at a phosphate concentration of 0.153 M is linear, and the half-life is 54.3 h; the plot is given in the Supporting Information. The plot of the pseudo-first-order rates versus phosphate concentration is shown in Figure 9. The bimolecular rate constant is found to be  $1.40 \times 10^{-5} \text{ M}^{-1} \text{ s}^{-1}$   $[\text{PO}_4^{3-}]$ , 1% of the rate for GD.

**DFP Reaction.** DFP is commonly used as a simulant to substitute for GB and GD due to its similar chemistry and slightly lower toxicity.<sup>46</sup> The reactivity of DFP in phosphate solution was faster than in acetate buffer, but the presence of a pyro compound was not detected. The rate of reaction for DFP

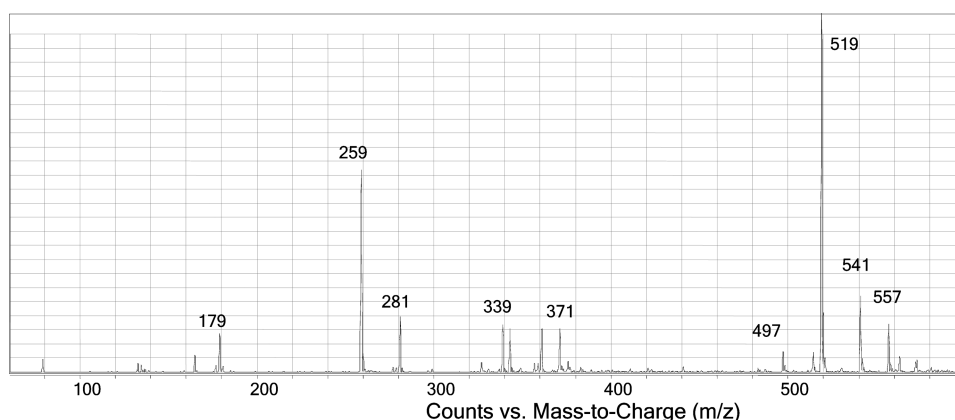


**Figure 8.** LC/MS of **2** using negative ion electrospray ionization. The  $[M-H]^-$  peak for the compound is at  $m/z$  259, and the  $m/z$  519 peak is the  $[2M-H]^-$  peak. It is interesting to observe alkali metal adducts at  $m/z$  281 for  $[M+Na-2H]^-$ ,  $m/z$  541 for  $[2M+Na-2H]^-$ , and  $m/z$  557 is  $[2M+K-2H]^-$ .

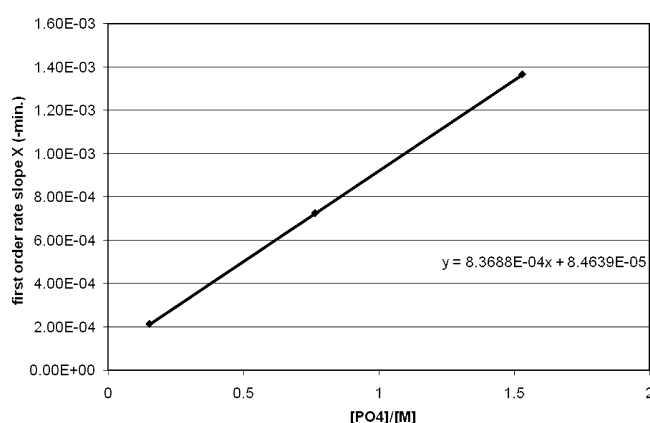


**Figure 9.** Linear plot of the first-order rates of VX reaction versus concentration of phosphate.

was  $2.84 \times 10^{-3} \text{ min}^{-1}$  at a concentration of 0.153 M phosphate, compared to a rate of  $4.3 \times 10^{-2} \text{ min}^{-1}$  for GB and  $1.18 \times 10^{-2} \text{ min}^{-1}$  for GD. The rate for DFP is a factor of 4 slower than GD and a factor of 15 slower than GB.

**Secondary 1 Reaction.** The reaction rate of **1** was measured. Figure 10 shows the kinetic plot for the reaction of **1** as a function of time at two different concentrations of phosphate. The rate of reaction in 0.153 and 0.046 M solution of phosphate are similar. The half-lives for these concentrations are 23.8 and 28.0 h, respectively. The slopes for the half-lives shown in Figure 10 are for times  $>500$  min after the reaction begins, and the GB is undetectable by this time, so **1** is no longer forming. These results indicate that the secondary reaction of **1** is not significantly dependent on the phosphate concentration, but is likely to be a hydrolysis reaction with water.

Simple modeling calculations of the kinetics of formation and reaction of **1** were done, and sample plots are shown in the Supporting Information. Rate constants that have been reported from the regression plots are consistent with modeling calculations of the concentration of **1** over the entire time range. The most complex case was the rate of reaction in the 0.0153 M solution shown in Figure 2. The loss of GB is much slower, and the concentration of **1** is almost flat to 14 000 min, and this reaction was difficult to model due to the changing rates as the pH values changed.

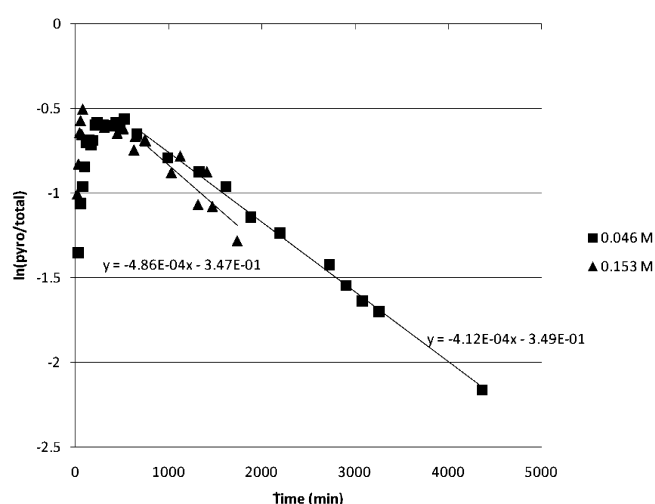


**Figure 10.** Semilog plot of the first-order rates of **1** reaction versus time for two concentrations of phosphate. The half-lives, calculated from the slope of the line for times after 500 min when the product is no longer forming, are 28.0 h for 0.046 M solution and 23.8 h for 0.153 M solution. Kinetic modeling of the data is given in the Supporting Information.

Gäb and co-workers say that their data supports a zero-order reaction rate for the decomposition of the pyro compounds.<sup>32</sup> However, a zero-order rate does not make theoretical sense under these conditions, and the present data is not consistent with a zero-order rate law. A plot is shown in the Supporting Information from the kinetic model that shows that the concentration decrease appears to be linear (zero-order) over the time range that was studied in that work, but it is first-order over a longer time.

The rate of reaction of **2** is similar to the rate for **1**, with a half-life of 37 h. The uncertainty is large because the signal-to-noise ratio of the NMR spectra is low because the signal is split into many peaks. The branching ratio is 1:0.66 for the products GD acid and **2**, respectively, for a phosphate concentration of 0.0766 M.

## DISCUSSION

Although this work has been done in synthetic phosphate buffer solution, biological matrices are also phosphate buffers that are near neutral pH. Standards for biological studies are

often prepared in phosphate buffers, so it may be necessary to be aware of the stability of nerve agent in such solutions containing phosphate. Interactions of nerve agents with phosphate could affect the reaction of nerve agents in biological solutions such as blood or standards made for biological studies.

It may be possible to monitor biological fluids for compounds **1** and **2** as a method for determining whether individuals have been exposed to nerve agent, as an alternative to current methods.<sup>47</sup> However, the concentration of orthophosphate in blood is rather low (1–2 mM) and undergoes complex reactions,<sup>48</sup> so the reactions with GB or GD in blood would be slow and may be overwhelmed by other loss mechanisms. Since the product compounds continue to react, the monitoring would be necessary within days after the exposure. The products of a reaction are likely to be difficult to find, due to binding with proteins and the complex matrix.

The toxicity of **1** and **2** are unknown, but they may have anticholinesterase activity, since the structures are similar to tetraethyl pyrophosphate, a cholinesterase inhibitor (oral LC<sub>50</sub> in rats of 500 µg/kg<sup>49</sup>). As a result, it is not possible to say that the GB or GD has been detoxified by the reaction with phosphate without testing of the toxicity of the reaction product. The possible product toxicity as well as the slow speed of the reactions will probably limit the application of these reactions to routine nerve agent decontamination.

The mechanism of the reaction has not been determined. The fact that the branching ratio of the reactions to form **1** and GB acid does not change as a function of phosphate concentration indicates that both products arise from a common intermediate involving a phosphate complex that decomposes to both products. There is a direct hydrolysis reaction of GB involving only water, which may be acid or base catalyzed, but it is much slower. The phosphate acts in a catalytic role to consume the nerve agent, for the reaction channel that produces the corresponding acid. There is no direct evidence about the structure of the reactive intermediate, in particular whether the P–F bond (or P–S for VX) is eliminated before or after the intermediate is formed. However, these results indicate that the destruction of toxic nerve agents can be accomplished in a catalytic way. Further research in this area of the fundamental chemistry of this class of compounds may assist in improving the reactivity.

## ■ ASSOCIATED CONTENT

### ■ Supporting Information

The Supporting Information includes additional kinetic plots, and a discussion of numerical kinetic modeling of the change of the concentration of the **1** and **2** products. This information is available free of charge via the Internet at <http://pubs.acs.org>.

## ■ AUTHOR INFORMATION

### Corresponding Author

\*E-mail: [william.r.creasy.ctr@us.army.mil](mailto:william.r.creasy.ctr@us.army.mil).

### Notes

The authors declare no competing financial interest.

## ■ ACKNOWLEDGMENTS

The authors thank H. Dupont Durst and E. Michael Jakubowski for support and helpful discussions. The work was performed at the Edgewood Chemical Biological Center

under Contract Numbers DAAD13-03-D-0017 and W911SR-10-D-0004.

## ■ REFERENCES

- (1) Epstein, J.; Callahan, J. J.; Bauer, V. E. The Kinetics and Mechanisms of Hydrolysis of Phosphonothiolates in Dilute Aqueous Solution. *Phosphorus* **1974**, *4*, 157–63.
- (2) Somani, S. M., ed. *Chemical Warfare Agents*; Academic: San Diego, CA, 1992.
- (3) Organization for the Prohibition of Chemical Weapons Web Page. "Nerve Agents," from *A FOA Briefing Book on Chemical Weapons: Threat, Effects, and Protection*. <http://www.opcw.org/resp/html/nerve.html>.
- (4) Munro, N. B.; Talmage, S. S.; Griffin, G. D.; Waters, L. C.; Watson, A. P.; King, J. F.; Hauschild, V. The Sources, Fate, and Toxicity of Chemical Warfare Agent Degradation Products. *Environ. Health Perspect.* **1999**, *107*, 933–74.
- (5) Larsson, L. The Alkaline Hydrolysis of Isopropoxy-methylphosphoryl Fluoride (Sarin) and Some Analogues. *Acta Chem. Scand.* **1957**, *11*, 1131–42.
- (6) Lohs, K. *Synthetische Gifte (Synthetic Poisons)*; Ministerium für nationale Verteidigung: Berlin, 1963; p 308.
- (7) Epstein, J.; Bauer, V. E.; Saxe, M.; Demek, M. M. The Chlorine-Catalyzed Hydrolysis of Isopropyl Methylphosphonofluoridate (Sarin) in Aqueous Solution. *J. Am. Chem. Soc.* **1956**, *78*, 4068–4071.
- (8) Franke, S. *Manual of Military Chemistry: Chemistry of Chemical Warfare Agents*; National Technical Information Service # AD-849 866, 1967; Vol. 1.
- (9) Epstein, J.; Cannon, P. L., Jr.; Sowa, J. R. The Catalysis of the Hydrolysis of Isopropyl Methylphosphonofluoridate in Aqueous Solutions by Primary Amines. *J. Am. Chem. Soc.* **1970**, *92*, 7390–93.
- (10) Epstein, J.; Rosenblatt, D. H. Kinetics of Some Metal Ion-Catalyzed Hydrolyses of Isopropyl Methylphosphonofluoridate (GB) at 25°C. *J. Am. Chem. Soc.* **1958**, *80*, 3596–98.
- (11) Epstein, J.; Rosenblatt, D. H.; Demek, M. M. Kinetics of the Reaction of Isopropyl Methylphosphonofluoridate with Catechols at 25°C. *J. Am. Chem. Soc.* **1956**, *78*, 341–43.
- (12) Epstein, J.; Plapinger, R. E.; Michel, H. O.; Cable, J. R.; Stephani, R. A.; Hester, R. J.; Billington, C., Jr.; List, G. R. Reactions of Isopropyl Methylphosphonofluoridate with Substituted Phenols. I. *J. Am. Chem. Soc.* **1964**, *86*, 3075–84.
- (13) Epstein, J.; Michel, H. O.; Rosenblatt, D. H.; Plapinger, R. A.; Stephani, R. A.; Cook, E. Reactions of Isopropyl Methylphosphonofluoridate with Substituted Phenols. II. *J. Am. Chem. Soc.* **1964**, *86*, 4959–63.
- (14) Davisson, M. L.; Love, A. H.; Vance, A.; Reynolds, J. G. *Environmental Fate of Organophosphorus Compounds Related to Chemical Weapons*; Lawrence Livermore National Laboratory, UCRL-TR-209748, 2005.
- (15) Boone, C. M. *Present State of CBRN Decontamination Methodologies*; TNO Report TNO-DV-2007-A028; Organisation for Applied Scientific Research (TNO) Defence, Security and Safety: Rijswijk, The Netherlands, 2007. This document is available from <http://stinet.dtic.mil>.
- (16) Wagner, G.; Yang, Y.-C. Rapid Nucleophilic/Oxidative Decontamination of Chemical Warfare Agents. *Ind. Eng. Chem. Res.* **2002**, *41*, 1925–1928.
- (17) Wagner, G. W.; Sorrick, D. C.; Procell, L. R.; Brickhouse, M. D.; Mcvey, I. F.; Schwartz, L. I. Decontamination of VX, GD, and HD on a Surface Using Modified Vaporized Hydrogen Peroxide. *Langmuir* **2007**, *23*, 1178–1186.
- (18) Waysbort, D.; McGarvey, D. J.; Creasy, W. R.; Morrissey, K. M.; Hendrickson, D. M.; Durst, H. D. A Decontamination System for Chemical Weapons Agents Using a Liquid Solution on a Solid Sorbent. *J. Hazard. Mater.* **2008**, *161*, 1114–1121.
- (19) Wang, A. A.; Mulchandani, A.; Chen, W. Specific Adhesion to Cellulose and Hydrolysis of Organophosphate Nerve Agents by a Genetically Engineered *Escherichia coli* Strain with a Surface-



Expressed Cellulose-Binding Domain and Organophosphorus Hydrolase. *Appl. Environ. Microbiol.* **2002**, 68, 1684–89.

(20) Gopal, S.; Rastoqi, V.; Ashman, W.; Mulbry, W. Mutagenesis of Organophosphorus Hydrolase to Enhance Hydrolysis of the Nerve Agent VX. *Biochem. Biophys. Res. Commun.* **2000**, 279, 516–19.

(21) Vayron, P.; Renard, P.-Y.; Taran, F.; Cr  minon, C.; Frob  rt, Y.; Grassi, J.; Mioskowski, C. Toward Antibody-Catalyzed Hydrolysis of Organophosphorus Poisons. *Proc. Natl. Acad. Sci. U.S.A.* **2000**, 97, 7058–7063.

(22) Tucker, M. D.; Comstock, R. H. Decontamination Formulation with Sorbent Additive, U.S. Patent #7,282,470, October 16, 2007 Tucker, M. D. Granulated Decontamination Formulations, U.S. Patent #7,276,468, October 2, 2007.

(23) Hoffman, D. M.; McGuire, R. R. Oxidizer Gels for Detoxification of Chemical and Biological Agents, U.S. Patent # 6,455,751, September 24, 2002.

(24) Hoffman, D. M.; Chiu, I. L. Solid-Water Detoxifying Reagents for Chemical and Biological Agents, U.S. Patent # 7,030,071, April 18, 2006.

(25) McDonald, W. F.; Parsons, A. B.; Northrup, V. M.; Hill-Clark, D.; O'Loughlin, M. E. *Developments of New Reactive Sorbents*, Battelle, Dec. 1993, Edgewood Research, Development, and Engineering Center Report ERDEC-CR-037.

(26) Bartelt-Hunt, S. L.; Barlaz, M. A.; Knappe, D. U. R.; Kjeldsen, P. Fate of Chemical Warfare Agents and Toxic Industrial Chemicals in Landfills. *Environ. Sci. Technol.* **2006**, 40 (13), 4219–4225.

(27) Bizzigotti, G. O.; Castelly, H.; Hafez, A. M.; Smith, W. H. B.; Whitmire, M. T. Parameters for Evaluation of the Fate, Transport, and Environmental Impacts of Chemical Agents in Marine Environments. *Chem. Rev.* **2009**, 109 (1), 236–256.

(28) Brevett, C. A. S.; Sumpter, K. B.; Nickol, R. G. Kinetics of the Degradation of Sulfur Mustard on Ambient and Moist Concrete. *J. Hazard. Mater.* **2009**, 162 (1), 281–291.

(29) Wagner, G. W.; O'Connor, R. J.; Edwards, J. L.; Brevett, C. A. S. Effect of Drop Size on the Degradation of VX in Concrete. *Langmuir* **2004**, 20, 7146–7150.

(30) Morrissey, K.; Schenning, A.; Fouse, J.; Smith, P.; Nunes, R.; Sumpter, K.; Durst, H. D. *Degradation of Chemical Warfare Agents in Potable Waters*; 2009 Chemical and Biological Defense Science and Technology Conference, Dallas, TX, Nov. 16–20, 2009.

(31) Kim, K.; Tsay, O. G.; Atwood, D. A.; Churchill, D. G. Destruction and Detection of Chemical Warfare Agents. *Chem. Rev.* **2011**, 111, 5345–5403.

(32) G  b, J.; John, H.; Blum, M.-M. Formation of Pyrophosphate-Like Adducts from Nerve Agents Sarin, Soman, and Cyclosarin in Phosphate Buffer: Implications for Analytical and Toxicological Investigations. *Toxicol. Lett.* **2011**, 200, 34–40.

(33) Grunwald, J.; Raveh, L.; Doctor, B. P.; Ashani, Y. Huperzine A as a Pretreatment Candidate Drug against Nerve Agent Toxicity. *Life Sci.* **1994**, 54 (14), 991–997.

(34) Broomfield, C. A.; Lenz, D. E.; MacIver, B. the Stability of Soman and Its Stereoisomers in Aqueous Solution: Toxicological Considerations. *Arch. Toxicol.* **1986**, 59, 261–265.

(35) Buckles, L. C. *The Hydrolysis Rate of GD*; Technical Command Informal Report TCIR 373, March 28, 1947.

(36) Yang, Y.-C.; Baker, J. A.; Ward, J. R. Decontamination of Chemical Warfare Agents. *Chem. Rev.* **1992**, 92, 1729–1743.

(37) Yang, Y.-C. Chemical Detoxification of Nerve Agent VX. *Acc. Chem. Res.* **1999**, 32, 109–115.

(38) Creasy, W. R.; Fry, R. A.; McGarvey, D. J. *Reaction of Nerve Agents with Phosphate Buffer at pH 7*, presented at the 2008 Chemical and Biological Defense Physical Science and Technology Conference, New Orleans, LA, 17–21 November 2008.

(39) Van Geet, A. L. Temperature Measurement in Nuclear Magnetic Resonance with a Spinning Thermistor. *Rev. Sci. Instrum.* **1969**, 40, 177–178.

(40) ACD/XNMR, v. 14.00; Advanced Chemistry Development, Inc.: Toronto, Canada, 2012.

(41) Yang, Y.-C.; Szafraniec, L. L.; Beaudry, W. T.; Rohrbaugh, D. K.; Procell, L. R.; Samuel, J. B. Autocatalytic Hydrolysis of V-Type Nerve Agent. *J. Org. Chem.* **1996**, 61, 8407–8413.

(42) The Supporting Information of ref 41 discusses the splitting of the VX pyro peaks as due to diastereomeric isomers, due to the two chiral P atoms in the compound. However, **1** has a similar splitting but only has one chiral P center. The software in ref 40 calculates coupling, not shifts from diastereomers, and it is in good agreement to the splitting. As a result, we conclude that the splittings for **1** are from P–P coupling, and the similar VX pyro splitting may also not be from diastereomers.

(43) Ellin, R. I.; Groff, W. A.; Kaminkis, A. The Stability of Sarin and Soman in Dilute Aqueous Solutions and the Catalytic Effect of Acetate Ion. *J. Environ. Sci. Health* **1981**, B16 (6), 713–717.

(44) Reference 32 does not report rate constants, but the effective rate constant of [GB] reaction can be obtained from the data provided using the pseudofirst order rate equation:  $[GB]_t = [GB]_0 \exp(-kt)$ , so  $k = -t^{-1} \ln([GB]_0 - \Delta[GB])/[GB]_0$ .  $[GB]_0 = 7.1$  mM, and  $\Delta[GB] = 83.6$   $\mu$ M/min, adding the corrected rates of reaction from both adduct formation and acid formation.

(45) Reference 34 gives a half-life of 6.6 h at 0.02 M phosphate in pH 7.4 buffered saline solution at 27  $^{\circ}$ C, which gives a rate constant of  $1.75 \times 10^{-3}$   $M^{-1} \text{ min}^{-1}$ .

(46) McGarvey, D. J.; Creasy, W. R.; Fry, R. A.; Durst, H. D. *Comparisons of Reactivity of Chemical Weapons Agents to Agent Simulants*, 238th American Chemical Society National Meeting, Washington, D.C., Aug. 16–20, 2009.

(47) Renner, J. A.; Dabisch, P. A.; Evans, R. A.; McGuire, J. M.; Totura, A. L.; Jakubowski, E. M.; Thomson, S. A. Validation and Application of a GC-MS Method for Determining Soman Concentration in Rat Plasma Following Low-Level Vapor Exposure. *J. Anal. Toxicol.* **2008**, 32, 92–98.

(48) Shoemaker, D. G.; Bender, C. A.; Gunn, R. B. Sodium-Phosphate Cotransport in Human Red Blood Cells. *J. Gen. Physiol.* **1988**, 92, 449–474.

(49) U.S. Department of Labor Occupational Safety and Health Administration Web Page, Occupational Safety and Health Guideline for Tetraethyl Pyrophosphate (TEPP), <http://www.osha.gov/SLTC/healthguidelines/tepp/recognition.html#healthhazard>.